International Journal of Pharmaceutics: X 1 (2019) 100006

Contents lists available at ScienceDirect

International Journal of Pharmaceutics: X

journal homepage: www.journals.elsevier.com/international-journal-of-pharmaceutics-x

Modulation of the fate of zein nanoparticles by their coating with a Gantrez® AN-thiamine polymer conjugate

Laura Inchaurraga[a], Ana L. Martínez-López[a], Muthanna Abdulkarim[b], Mark Gumbleton[b], Gemma Quincoces[c], Ivan Peñuelas[c], Nekane Martin-Arbella[a], Juan M. Irache[a,*]

[a] NANO-VAC Research Group, Department of Chemistry and Pharmaceutical Technology, University of Navarra, Spain
[b] School of Pharmacy and Pharmaceutical Sciences, Cardiff University, Cardiff, UK
[c] Radiopharmacy Unit, Department of Nuclear Medicine, Clinica Universidad de Navarra, University of Navarra, Spain

ARTICLE INFO

Keywords:
Zein
Nanoparticles
Thiamine
Oral delivery
Coating
Mucus permeating

ABSTRACT

The aim of this work was to evaluate the mucus-permeating properties of nanocarriers using zein nanoparticles (NPZ) coated with a Gantrez® AN-thiamine conjugate (GT). NPZ were coated by incubation at different GT-to-zein ratios: 2.5% coating with GT (GT-NPZ1), 5% (GT-NPZ2) and 10% (GT-NPZ3). During the process, the GT conjugate formed a polymer layer around the surface of zein nanoparticles. For GT-NPZ2, the thickness of this corona was estimated between 15 and 20 nm. These nanocarriers displayed a more negative zeta potential than uncoated NPZ. The diffusivity of nanoparticles was evaluated in pig intestinal mucus by multiple particle tracking analysis. GT-NPZ2 displayed a 28-fold higher diffusion coefficient within the mucus layer than NPZ particles. These results align with *in vivo* biodistribution studies in which NPZ displayed a localisation restricted to the mucus layer, whereas GT-NPZ2 were capable of reaching the intestinal epithelium. The gastro-intestinal transit of mucoadhesive (NPZ) and mucus-permeating nanoparticles (GT-NPZ2) was also found to be different. Thus, mucoadhesive nanoparticles displayed a significant accumulation in the stomach of animals, whereas mucus-penetrating nanoparticles appeared to exit the stomach more rapidly to access the small intestine of animals.

1. Introduction

In 1982, the Food and Drug Administration (FDA) approved the first commercially-available recombinant protein for the treatment of diabetic patients (Leader et al., 2008). Three decades after the approval of recombinant insulin, more than 239 different therapeutic proteins and peptides have been approved for clinical use (Lau and Dunn, 2018; Usmani et al., 2017). Peptides and proteins offer a higher specificity and potency as well as a lower interference with normal biological processes than conventional small-molecule drugs (Mitragotri et al., 2014; Skalko-Basnet, 2014). In general, all of these compounds are administered as a parenteral injection. However, the inherent short half-lives of these biomacromolecules require frequent administrations that may compromise patient compliance and, thus, restrict their therapeutic value, particularly for chronic diseases (Remington et al., 2013; Shah et al., 2016).

In the last decades, enormous research efforts have been devoted to the development of formulation strategies for the oral delivery of these compounds. The oral administration of proteins and peptides is attractive for many patients due to the absence of pain and discomfort associated to injections (Muheem et al., 2016). In addition, from a technological point of view, the manufacture of oral medicines does not require particular facilities, process or containers to produce and maintain sterile conditions. In addition, for certain polypeptides, such as insulin or indeed incretin mimetics such as exenatide, the oral delivery route is more closely mimics the physiological process (Fonte et al., 2013). The oral delivery of proteins and peptides remains an important challenge with many developmental issues to solve. The physico-chemical properties (i.e., MW, hydrophilic character or presence of ionisable functional groups) and enzymatic sensitivity strongly hamper the absorption of therapeutic proteins and peptides. As a consequence, their oral bioavailability (in general) is really low (< 1%) (Muheem et al., 2016; Yin et al., 2014).

In order to solve these drawbacks, the use of biodegradable nanoparticles has been proposed. In principle, these pharmaceutical dosage forms may encapsulate the therapeutic compound and, thus, offer protection against its eventual hydrolytic or enzymatic degradation. In addition, and due to their matrix structure, these nanoparticles may

* Corresponding author at: Dep. Chemistry and Pharmaceutical Technology, University of Navarra, C/Irunlarrea, 1, 31008 Pamplona, Spain.
E-mail address: jmirache@unav.es (J.M. Irache).

https://doi.org/10.1016/j.ijpx.2019.100006
Received 29 November 2018; Received in revised form 9 January 2019; Accepted 11 January 2019
Available online 25 January 2019

control the release of the cargo. However, in many cases, these devices possess mucoadhesive properties and remain trapped in the protective mucus layer covering the gut epithelium (Ensign et al., 2012; Lai et al., 2009). In the particular case of protein and peptide delivery, this may be an important limitation with greater exposure of any released polypeptide to the digestive enzymes localized in the luminal space adjacent to the glycocalyx covering the surface of enterocytes (Bruno et al., 2013; Maher et al., 2016). In addition, mucoadhesive properties of nanoparticles limits their residence time within the gut mucosa which will be determined by the mucus turn-over (Dawson et al., 2004; Lai et al., 2009). The use mucus-permeating nanocarrier has been suggested as an alternative to minimize such issues.

In order to generate these devices, different alternatives have been proposed, including the use of immobilized proteolytic enzymes on the surface of the nanocarriers (Pereira de Sousa et al., 2015), the co-encapsulation of mucolytic agents (Netsomboon and Bernkop-Schnürch, 2016), or the design of zeta potential changing systems (Perera et al., 2015). Another possibility may be the use of "slippery" nanoparticles which possess a highly-dense hydrophilic coat shielding hydrophobic interactions between the nanoparticles and the components of the mucus and facilitating passage through this mucus biopolymer. The coating of nanoparticles with poly(ethylene glycol) (Inchaurraga et al., 2015; Li et al., 2001) or surfactants such as Pluronic®F 127 (Schneider et al., 2017) has also explored, as the use of surfactant- based micellar drug delivery systems (Menzel et al., 2018).

In this context, the aim of this work was to develop and evaluate the mucus-permeating properties of nanocarriers based on the coating of zein nanoparticles with a Gantrez® AN-thiamine conjugate. Zein is a Generally Recognised as Safe (GRAS) material that, due to its amphiphilic character, can easily interact with a wide group of compounds, including proteins (Cserháti and Forgács, 2005). Significantly, nanoparticles based on the conjugate between Gantrez® AN and thiamine have demonstrated the capability to reach the intestinal epithelium minimizing their retention in the protective mucus gel layer (Inchaurraga et al., 2019).

2. Materials and methods

2.1. Materials

The copolymer of methylvinylether and maleic anhydride or poly (anhydride) (Gantrez® AN 119) was supplied by Ashland Inc. (Barcelona, Spain). Thiamine hydrochloride, zein, mannitol, lysine, agarose, glutaraldehyde, propylene oxide, sodium cacodylate and EPON™ were purchased from Sigma-Aldrich (Madrid, Spain). Ethanol were provided by Panreac (Barcelona, Spain). Acetone was obtained from VWR-Prolabo, (Linars del Vallès, Spain). Perylene-Red (BASF Lumogen® F Red 305) was from Kremer Pigmente GmbH & Co. (Aichstetten, Germany) and OCT™ Compound Tissue-Tek from Sakura Finetek Europe (Alphen aan Der Rijn, The Netherlands). 4′,6-diamidino-2-phenylindole (DAPI) was obtained from Biotium Inc. (Madrid, Spain). Glass bottom imaging dishes (35 mm diameter dish with a glass coverslip at 1.5 mm thick and 10 mm diameter) were from MatTek Corporation (Ashland, USA). PLGA nanoparticles (PDLG-5002 containing lactic:glycolic at 50%:50%, MW 17 KDa.) with a mean size of 161 ± 0.03 nm and a zeta potential of −29.2 ± 2.11, were supplied by Nanomi B.V. (Oldenzaal, The Netherlands).

2.2. Mucus

Freshly isolated pig intestinal ileum (2 m in length from proximal region) was obtained from a local abattoir (Cardiff, UK) and kept in ice-cold oxygenated phosphate buffered saline (PBS) (no longer than 2 h) prior to sample processing. The ileum was processed into 25 cm lengths with each length incised longitudinally to allow intestinal food and other waste debris to be was gently rinsed away by ice-cold PBS. The mucus was then harvested using by an approach that optimized the yield of the loose mucus layer but critically also a significant amount of the adherent mucus layer (Cone, 2009). The intestinal surface was gently scraped by spatula which limits the shedding of intestinal epithelial tissue. Mucus was divided into aliquots (0.5 g) and kept at −20 °C prior to experimentation (Larhed et al., 1998).

2.3. Preparation of Gantrez® AN-thiamine conjugate (GT)

The conjugate was created by the covalent binding of thiamine to the poly(anhydride) backbone (Inchaurraga et al., 2019). To achieve this, 5 g Gantrez® AN were dissolved in 200 mL acetone. Then, 125 mg thiamine was added and the mixture was heated at 50 °C, under magnetic agitation at 400 rpm, for 3 h. The mixture was filtered through a pleated filter paper and the organic solvent was eliminated under reduced pressure in a Büchi R-144 apparatus (BÜCHI Labortechnik AG, Flawil, Switzerland). Finally, the resulting powder was stored at room temperature. The conjugate was named GT.

2.4. Preparation of zein nanoparticles coated with the Gantrez® AN-thiamine conjugate (GT-NPZ)

Zein nanoparticles were prepared by a desolvation procedure (Peñalva et al., 2015) and then coated with the synthesized Gantrez® AN-thiamine conjugate. The resulting nanoparticles were purified, concentrated and, finally, dried. In brief, 200 mg zein and 30 mg lysine were dissolved in 20 mL ethanol 55% and incubated under agitation at RT for 15 min. In parallel, a 2% aqueous solution of the Gantrez® AN-thiamine conjugate was prepared by dispersing the polymer in purified water till complete solubilisation. Nanoparticles were obtained after the addition of 20 mL purified water to the hydroalcoholic solution of zein and lysine. Then, a determined volume of GT solution (0.25, 0.5 or 1 mL) was added and the mixture was maintained under agitation at RT for 30 min. The resulting suspension of nanoparticles was purified and concentrated down to 20 mL by ultrafiltration through a polysulfone membrane cartridge of 500 kDa pore size (Medica SPA, Medolla, Italy). Finally, 10 mL of a mannitol aqueous solution (4% w/v) was added to the suspension of nanoparticles and the mixture was dried in a Büchi Mini Spray Drier B-290 apparatus (Büchi Labortechnik AG, Switzerland). The following parameters were selected: inlet temperature of 90 °C, outlet temperature of 60 °C, spray-flow of 600 L/h, and aspirator at 100% of the maximum capacity. The zein coated nanoparticles were named as GT-NPZ.

As control, "naked" zein nanoparticles (NPZ) were prepared in the same way as described above but in the absence of GT.

For different *in vitro* and *in vivo* studies, fluorescently labeled nanoparticles were used. Here, 2.5 mL of a 0.04% Lumogen®F red 305 solution in pure ethanol was added to the hydroalcoholic solution containing zein and lysine. The mixture was maintained under agitation. Then, the nanoparticles were prepared, purified and dried as described above.

2.5. Preparation of poly(anhydride) nanoparticles (PA-NP)

Nanoparticles based on Gantrez®AN (PA-NP) were prepared as described previously (Ojer et al., 2010) and employed as control of mucoadhesive nanoparticles. Briefly, 400 mg Gantrez® AN were dissolved in 20 mL acetone. The nanoparticles were formed by the addition of 40 mL ethanol followed of the addition of 40 mL purified water. The organic solvents were eliminated under reduced pressure, purified by centrifugation at 5000 × g for 20 min (SIGMA Lab. centrifuges, Osterode am Harz, Germany) using dialysis tubes Vivaspin® 300,000 MWCO (Sartorius AG, Madrid, Spain) and, finally dried by Spray-drying. The nanoparticles displayed a size of 213 ± 2 nm and a zeta potential of −53 ± 2 mV.

2.6. Characterization of nanoparticles

2.6.1. Particle size, zeta potential and yield

The particle size, polydispersity index (PDI) and zeta-potential were determined by photon correlation sprectroscopy (PCS) and electrophoretic laser Doppler anemometry respectively, using a Zetasizer analyser system (Brookhaven Instruments Corporation, New York, USA). The diameter of the nanoparticles was determined after dispersion in ultrapure water (1/10) and measured at 25 °C by dynamic light scattering angle of 90°. The zeta potential was determined as follows: 200 µL of the samples were diluted in 2 mL of a 0.1 mM KCl solution adjusted to pH 7.4.

In order to quantify the amount of protein transformed into nanoparticles, 10 mg of the nanoparticle formulation was dispersed in water and centrifuged at 17.000 × g for 20 min. Supernatants were discarded and the pellets were digested with ethanol 75%. Then, the amount of protein was quantified by UV spectrophotometry at 278 nm in an Agilent 8453 system (Agilent Technologies, USA). For analysis, calibration curves were constructed between 90 and 1200 µg/mL (R^2 greater than 0.999; quantitation limit = 143 µg/mL). The amount of protein forming nanoparticles in the formulation was estimated as the ratio between the amount of the protein quantified in the pellet of the centrifuged samples and the total amount of protein used for the preparation of nanoparticles and expressed in percentage.

2.7. Morphology and shape

The morphology and shape of nanoparticles were evaluated by TEM. In brief, 20 mg of the spray dried powder containing the nanoparticles were dispersed in 2 mL cacodylate 0.1 M containing glutaraldehyde 4%. After one hour of incubation, nanoparticles were centrifuged at 100 × g (5 min). The pellet was resuspended in 2 mL water and centrifuged again. Then, 2 mL of osmium 1% was added to the nanoparticles and kept at 4 °C for 1 h. The excess of osmium was eliminated by centrifugation at 100 × g for 5 min. Nanoparticles were resuspended in 2 mL water and centrifuged again. Then, 200 µL of agarose 2% were added to the nanoparticles, vortexed for 1 min and kept at 4 °C overnight. From this sample, 1 mL was inserted into an embedding flask and dehydrated with ethanol of increasing graduation for 3 h. Then, gelatin capsules were filled with a solution of propylene oxide-EPON™ (1:1) and the samples were inserted. These capsules were incubated at increasing temperatures (37 °C, 45 °C and 60 °C) for the polymerization of the EPON™. Finally, 50–70 nm sections of the samples were obtained with a Leica Ultracut R ultramicrotome (Wetzlar, Germany). The sections were placed in a copper grid and treated with 3% uranil acetate-lead for 5 min and completely dried at room temperature. For the visualization of nanoparticles, a Zeiss Libra 120 Transmission Electron Microscope (Oberkochen, Germany) coupled with a digital imaging system Gatan Ultrascan 1000 2 k × 2 k CCD was used.

2.8. Quantification of Lumogen® F red 305

The amount of Lumogen®F Red 305 red loaded in the nanoparticles was quantified by UV–Vis spectrometry at wavelength 580 nm (Labsystems iEMS Reader MF, Vantaa, Finland). For this purpose, the difference between its initial concentration added and the concentration found in the supernatant after the centrifugation of the samples in water (2800 × g for 20 min) was calculated. For quantification, standard curves of Lumogen®F Red in ethanol 75% were used (concentration range of 5–30 µg/mL; $R^2 \geq 0.999$).

2.9. Radiolabeling of nanoparticles with ^{99m}Tc

Nanoparticles were radiolabeled with technetium-99 m by reduction with stannous chloride as described (Areses et al., 2011). For this purpose, 0.8–1.0 mg nanoparticles were pre-tinned with 0.05 mg/mL of $SnCl_2$ and subsequently labelled for 30 min with 1–2 mCi of freshly eluted ^{99m}Tc-pertechnetate from ^{99}Mo-^{99m}Tc generator. The overall procedure was carried out in helium-purged vials. The radiochemical purity was analysed by radiochromatography (Whatman 3MM, NaCl 0.9%). The radiolabeling yield was always over 95%.

2.10. Multiple particle tracking (MPT) in mucus

The diffusion of nanoparticles through porcine intestinal mucus barrier was assessed by MPT technique (Abdulkarim et al., 2015; Rohrer et al., 2016). Samples (0.5 g) of porcine intestinal mucus were incubated in glass-bottom MatTek imaging dishes at 37 °C. The fluorescently labelled nanoparticles were inoculated into each 0.5 g mucus sample in a 25 µL aliquot at a suspension concentration of 0.002%. To ensure effective particle distribution following inoculation within the mucus, a 2 h period of equilibration was adopted prior the capture of nanoparticle movements by video microscopy. Video capture involved 2-dimensional imaging on a Leica DM IRB wide-field epifluorescence microscope (x63 magnification oil immersion lens) using a high speed camera (Allied Vision Technologies, Stadtroda, Germany) running at a frame rate of 33 ms i.e. capturing 30 frames sec^{-1}; each completed video film comprised 300 frames. For each 0.5 g mucus sample approximately 120 nanoparticles were simultaneously tracked and their movements captured. Videos were imported into Fiji ImageJ software to convert the movement of each nanoparticle into individual nanoparticles trajectories across the full duration of the 10 s videos. However, for the analysis of particle diffusion only a 30 frame video period (1 s) was used, with the criterion that any individual particle tracked must display a continuous presence in the X-Y plane 8 throughout the respective 30 sequential frames. The individual particle trajectories were converted into numeric pixel data (Mosaic Particle Tracker within Fiji ImageJ) which, based on the microscope and video capture settings, was converted into metric distance. The distances moved by every individual particle over a selected time interval (Δt) in the X-Y trajectory were then expressed as a squared displacement (SD). The mean square displacement (MSD) of any single particle (n) represents the geometric mean of that particle's squared displacements throughout its entire 30-frame trajectory. MSD was determined as follows (Macierzanka et al., 2014):

$$MSD_{(n)} = (X\Delta t)^2 + (Y\Delta t)^2 \quad (1)$$

For each nanoparticle type studied an "ensemble mean square displacement" (defined by $< MSD >$) was then determined for each of the three replicate studies. The Effective Diffusion Coefficient ($< Deff >$) for a particular nanoparticle type was then calculated by:

$$<Deff> = <MSD> / (4\Delta t) \quad (2)$$

where 4 is a constant relating to the 2-dimensional mode of video capture and Δt is the selected time interval.

The proportion of diffusive particles through the mucus matrix was evaluated by measuring particle diffusion across various time intervals (Lai et al., 2009). Eq. (3) was used to determine a Diffusivity Factor (DF) which expresses the effective diffusion coefficient for each individual particle (Deff) across the time intervals (Δt) of 1 and 0.2 s, when it is considered as Brownian motion.

$$DF = Deff\ \Delta\ t = 1sec/Deff\ \Delta\ t = 0.2\ sec \quad (3)$$

where the individual particle Deff = MSD/(4Δt). Particles with a DF value of 0.9 and greater were defined as diffusive. The proportion of the diffusive particles within a given NP type under study was then calculated and expressed as %Diffusive particles.

In parallel, the particles' diffusion coefficient (D°) in water was calculated by the Stokes-Einstein equation at 37 °C (Philibert, 2005). For this purpose, Eq. (4) was applied:

$$D^{\circ} = \kappa T / 6\pi\eta r \quad (4)$$

where k is Boltzmann constant, T is absolute temperature, η is water viscosity and r is radius of the particle.

The diffusion of all particles was also expressed as the parameter, % ratio [Deff]/[D°] which provided a measure of the relative efficiency of particle diffusion through mucus when particles' intrinsic free Brownian motion in water is taken into account. As such it affords comparison of particle diffusion in mucus after accounting for the impact of a particles' surface composition upon its unrestricted diffusion in solution. It is essentially a measure that more directly addresses the relative impact between particles of differing surface physico-chemical properties and the interactions, and the steric hindrance of the mucin network.

2.11. Gastro-intestinal transit studies with ^{99m}Tc-nanoparticles

These studies were carried out in female Wistar rats weighing 250–300 g. All the procedures were performed following a protocol previously approved by the "Ethical and Biosafety Committee for Research on Animals" at the University of Navarra in line with the European legislation on animal experiments.

Animals were lightly anaesthetised with 2% isoflurane gas for administration of nanoparticles (dispersed in 1 mL water) by oral gavage, and then quickly awakened. Each animal received one single dose of radiolabeled nanoparticles (1 mCi; 0.8–1.0 mg radiolabeled nanoparticles that were completed with up to 10 mg with unlabelled nanoparticles). SPECT/CT studies were performed three hours after administration of ^{99m}Tc-nanoparticles, animals were anaesthetised with 2% isoflurane gas and placed in prone position on the gamma camera (Symbia T2 Truepoint; Siemens Medical System, Malvern, USA). The acquisition parameters for SPECT studies were: 128 × 128 matrix, 90 images, 7 images per second and CT: 110 mAs and 130 Kv, 130 images, slice thickness 3 mm. Fused images were processed using the Syngo MI Applications TrueD software.

2.12. Biodistribution studies with fluorescently labeled nanoparticles

The tissue distribution of nanoparticles in the gastrointestinal mucosa was visualized by fluorescence microscopy. For that purpose, 25 mg of Lumogen® F Red-labeled nanoparticles were orally administered to rats as described above. Two hours later, animals were sacrificed by cervical dislocation and the guts were removed. Ileum portions of 1 cm were collected, cleaned with PBS, stored in the tissue proceeding medium OCT™ and frozen at −80 °C. Each portion was then cut into 5-μm sections on a cryostat and attached to glass slides. Finally, these samples were fixed with formaldehyde and incubated with DAPI (4′,6-diamidino-2-phenylindole) for 15 min before the cover assembly. The presence of both fluorescently loaded poly(anhydride) nanoparticles in the intestinal mucosa and the cell nuclei dyed with DAPI were visualized in a fluorescence microscope (Axioimager M1, Zeiss, Oberkochen, Germany) with a coupled camera (Axiocam ICc3, Zeiss, Oberkochen, Germany) and fluorescent source (HBO 100, Zeiss, Oberkochen, Germany). The images were captured with the software ZEN (Zeiss, Oberkochen, Germany). As control, a suspension of Lumogen® F Red 305 was administered.

3. Results

3.1. Preparation of GT-coated zein nanoparticles

The first approach was to optimize the coating process of zein nanoparticles. The influence of the GT-to-zein ratio on the physico-chemical properties of nanoparticles was evaluated (Table 1). As expected, by increasing the GT-to-zein ratio, the mean size and the negative zeta potential of the resulting nanoparticles increased. Under the experimental conditions tested, all the nanoparticle formulations displayed homogeneous characteristics with a PDI below 0.2. All the nanoparticles displayed negative surface charges, however, formulations presenting the GT coating showed slightly more negative surface charges than "naked" nanoparticles.

Table 1
Influence of the GT-to-zein ratio (expressed in percentage) on the physico-chemical properties of the resulting nanoparticles. Data expressed as mean ± SD (n = 3).

Formulation	GT-to-zein ratio (%)	Size (nm)	PDI	Zeta Potential (mV)
NPZ	0	235 ± 3	0.120 ± 0.014	−35 ± 4
GT-NPZ1	2.5	258 ± 2	0.091 ± 0.033	−45 ± 2
GT-NPZ2	5.0	271 ± 1	0.151 ± 0.016	−45 ± 3
GT-NPZ3	10	345 ± 8	0.182 ± 0.078	−55 ± 5

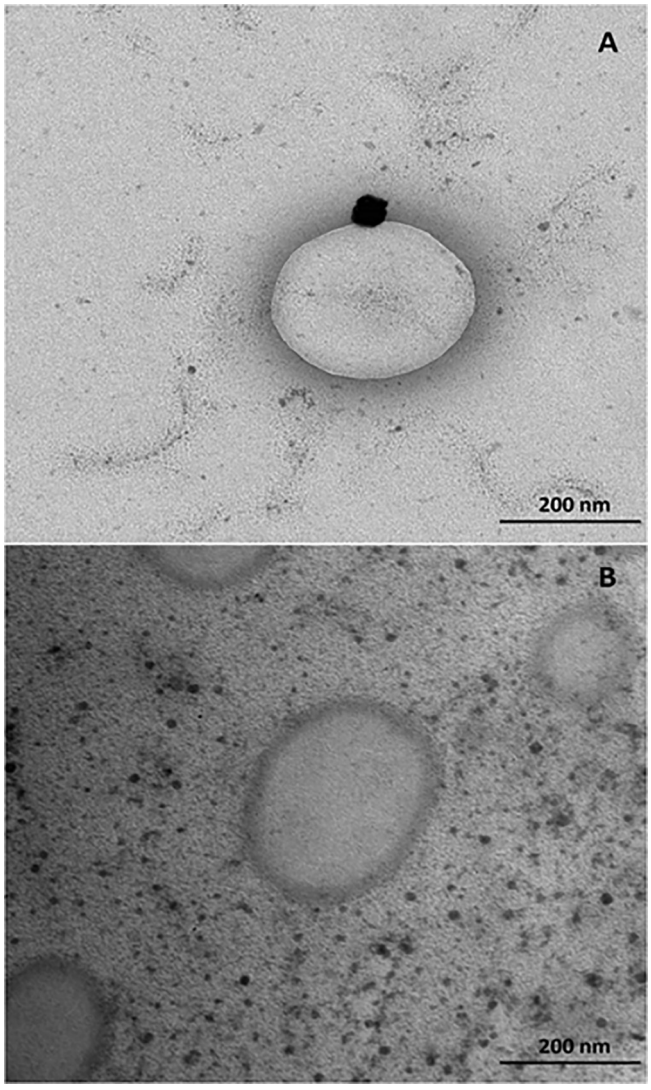

Fig. 1. Tomography electron microscopy of (A) "naked" zein nanoparticles (NPZ) and (B) GT-coated nanoparticles (GTZ-NP).

Fig. 1 shows TEM photographs of bare zein nanoparticles and zein nanoparticles coated with GT at a GT-to-zein ratio of 5% (GT-NPZ2). These nanocarriers displayed spherical shape and similar sizes to those obtained by photon correlation spectroscopy. Interestingly, coated nanoparticles showed a clear corona that was missing in uncoated zein nanoparticles. The thickness of this coating layer, covering the surface

Table 2
Diffusion behavior of the different formulations tested. Data expressed as mean ± SD (n = 3). D°: diffusion coefficient in water; < Deff > : diffusion coefficient in mucus; ratio % < Deff > /D°: relative efficiency of particles diffusion; R: ratio between the % < Deff > /D° for the different formulations tested and the % < Deff > /D° value for NPZ; PLGA-NP: PLGA nanoparticles; PA-NP: poly(anhydride) nanoparticles; NPZ: "naked" zein nanoparticles; GT-NPZ1: GT-coated zein nanoparticles at a GT-to-zein ratio of 2.5%; GT-NPZ2: GT-coated zein nanoparticles at a GT-to-zein ratio of 5%; GT-NPZ3: GT-coated zein nanoparticles at a GT-to-zein ratio of 10%.

Formulation	D° (water) cm^2. $S^{-1} \times 10^{-9}$	< Deff > (mucus) cm^2. $S^{-1} \times 10^{-9}$ Mean (± SD)	% < Deff > /D°	R
PLGA-NP	27.91	0.013 (± 0.008)	0.0005	0.06
PA-NP	20.71	0.00167 (± 0.096)	0.0081	0.91
NPZ	19.12	0.00171 (± 0.034)	0.0089	1.00
GT-NPZ1	17.42	0.00376 (± 0.095)	0.0216	2.42
GT-NPZ2	16.58	0.04129 (± 1.639)	0.2490	27.98
GT-NPZ3	13.03	0.00030 (± 0.006)	0.0023	0.26

of zein nanoparticles, was estimated to be between 15 and 20 nm.

3.2. Multiple particle tracking (MPT) in mucus

The influence of the GT-to-zein ratio used for the preparation of nanoparticles on the diffusion through porcine intestinal mucus was assessed by the MPT technique (Table 2). GT-coated nanoparticles at a GT-to-zein ratios of 2.5% (GT-NPZ1) and 5%, (GT-NPZ2) displayed higher ability to diffuse through the mucus than "naked" nanoparticles (NPZ). These bare NPZ particles showed a similar capacity to diffuse in mucus to that of the poly(anhydride) nanoparticles (PA-NP). The < Deff > of GT-NP 2.5% (GT-NPZ1) was 2.2-fold higher than NPZ, while the < Deff > of GT-NP 5% (GT-NPZ2) was 24-fold higher than bare zein nanoparticles. However, when the GT-to-zein ratio was increased up to 10% (GT-NPZ3), the ability of the nanoparticles to diffuse through the mucus significantly decrease, being even slower than uncoated nanoparticles and quite similar to PLGA-NP. In fact, GT-NPZ3 displayed an important tendency to form aggregates with mucus.

3.3. Gastro-intestinal transit studies with ^{99m}Tc-nanoparticles

Fig. 2 shows the comparison of the gastro-intestinal transit data of nanoparticles (radiolabeling with ^{99m}Tc) when administered by the oral route to laboratory animals. In all cases, 2 h post-administration, nanoparticles were localized in the stomach and the small intestine. Nanoparticles coated with GT appeared to transit faster through the gastro-intestinal tract than uncoated nanoparticles, as evidenced by more intense signal in the small intestine than in the stomach. The images in Fig. 2 show the intensity of the radioactivity in the stomach to be higher for NPZ than for GT-NPZ1 (data not shown) and GT-NPZ2. Surprisingly, GT-NPZ3 showed a significantly lower intensity of the radioactivity in the small intestine than GT-NPZ1 and GT-NPZ2. No activity was observed in the liver or the lungs indicating a lack of any measurable systemic availability of the oral administered particles.

3.4. Biodistribution studies with fluorescently labeled nanoparticles

Fig. 3 shows fluorescence microscopy images of ileum samples from animals treated with Lumogen® F Red-labelled nanoparticles. Control formulation (an aqueous suspension of the fluorescent marker) was visualized as large aggregates in the lumen or in contact with the external mucus layer (data not shown). Bare nanoparticles displayed a localisation mainly restricted to the mucus layer protecting the epithelium in the ileum (Fig. 3A and B). Conversely, for nanoparticles containing GT as coating material appeared capable of reaching the epithelium and interacting more widely with the intestinal cells

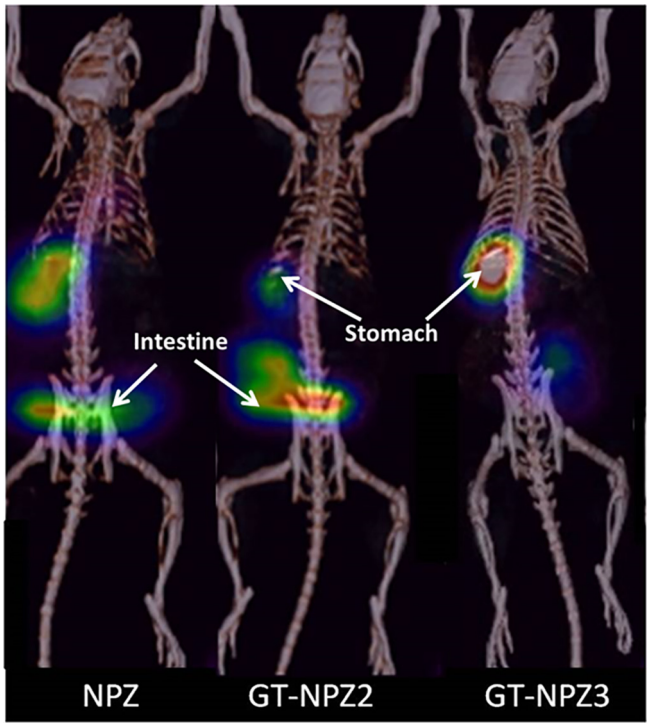

Fig. 2. Volume rendered fused SPECT-CT images from representative animals 2 h after administration of ^{99m}Tc-labelled NP by oral gavage. NPZ: "naked" nanoparticles; GT-NPZ2: Gantrez® AN-thiamine-coated zein nanoparticles at a GT/zein ratio of 5%; GT-NPZ3: Gantrez® AN -thiamine-coated zein nanoparticles at a GT/zein ratio of 10%.

(Fig. 3C–H). This interaction was higher for GT-NPZ2 than for GT-NPZ1 and GT-NPZ3.

4. Discussion

The objective of this work was to explore the effect of the coating of zein nanoparticles with a hydrophilic conjugate (based on the binding of thiamine to Gantrez® AN) on the mucoadhesive/mucus-penetrating properties of the resulting nanocarriers. When zein nanoparticles were coated with the GT conjugate, particle size increased as GT content increased (Table 1). This increasing in the size of coated nanoparticles was attributed to the formation of a polymer layer around the surface of zein nanoparticles (Fig. 1). As a consequence, for zein nanoparticles coated at a GT content of 5%, the mean particle size was ca. 11–15% higher than for uncoated ones. Additionally, the coatings increased the negative zeta potential compared to the bare nanoparticles. The incremental increases in surface negative charges were directly related to the presence of the conjugate on the surface of the nanoparticles. Indeed, the binding of thiamine to the polymer backbone (through the reaction and opening of the anhydride groups) would yield carboxylic acids susceptible of ionization (Inchaurraga et al., 2019). During the coating process, the hydrophobic portions of GT conjugate would interact with the hydrophobic areas of zein nanoparticles, whereas the hydrophilic thiamine groups and the carboxylic acids would remain oriented through the external layer of the nanocarriers in contact with the dispersant aqueous medium. This model concurs with Rouzes and co-workers, who proposed a similar mechanism to explain the disposition of an amphiphilic dextran derivative when adsorbed on poly (lactic acid) nanoparticles (Rouzes et al., 2000).

In order to study the capability of zein-based nanoparticles to diffuse through a mucus layer *in vitro*, we used the multiple particle tracking technique and intestinal pig mucus. In this study the different nanoparticles tested displayed negative zeta potentials and mean sizes

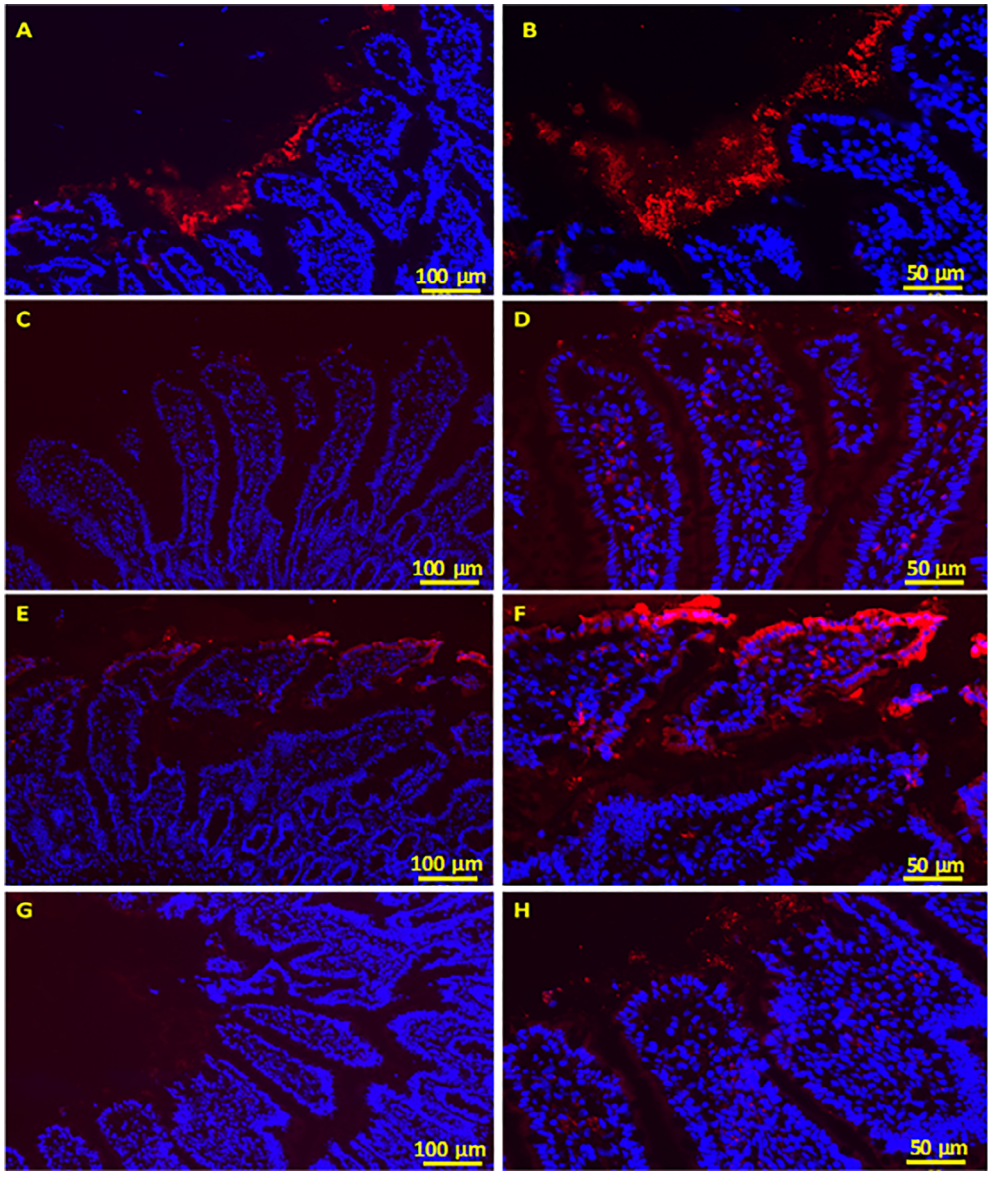

Fig. 3. Fluorescence microscopic visualisation of nanoparticles containing GT (GT-NPZ1, GT-NPZ2 and GT-NPZ3) and control ones (NPZ) in a longitudinal section of the ileum of rats 2 h post administration. A and B: NPZ; C and D: GT-NPZ1; E and F: GT-NPZ2; G and H: GT-NPZ3.

ranging from 160 nm (for control PLGA nanoparticles) till 350 nm (for GT-NPZ3). MPT studies revealed that the coating of zein nanoparticles with the Gantrez® AN-thiamine conjugate clearly modified their diffusion in intestinal pig mucus (Table 2). This is in line with previous observations describing that the capability of nanoparticles to pass through a network of intestinal mucus is highly dependent on the particle surface chemistry (Suk et al., 2011; Yildiz et al., 2015). PLGA nanoparticles, as expected, displayed a very poor capability to diffuse through the mucus. This finding aligns with previous works suggesting that the hydrophobic surface characteristics of PLGA nanoparticles would facilitate their interaction and binding with the hydrophobic domains of the mucin chains (Mert et al., 2012; Mura et al., 2011). For zein nanoparticles, their diffusivity in the mucus was found to be higher than for PLGA nanoparticles and similar to that of poly(anhydride) nanoparticles (Table 2), that have been defined as mucoadhesive nanocarriers (Arbós et al., 2003, 2002; Yoncheva et al., 2005). Interestingly, when zein nanoparticles were coated with GT (up to a GT-to-protein ratio of 5%), the diffusion of the resulting nanocarriers through mucus increased, and was very notable for GT-NPZ2 with a diffusion coefficient about 28-times higher than for bare nanoparticles.

When nanoparticles were coated with a GT-to-zein ratio of 10% (GT-NPZ3), their diffusivity in intestinal mucus diminished some 6-fold lower than that observed for bare zein nanoparticles. These nanoparticles displayed a tendency to form aggregates when mixed with mucus. Even when expressing mucus diffusion relative to that in water (i.e. normalizing for differences in particle size) the GT-NPZ3 particle were less efficient at permeating the mucus than NPZ (Table 2). This behavior could be associated with a highly dense GT coating in GT-NPZ3 that would result in a less flexible coating with entanglements between the poly(anhydride) chains that would facilitate their interaction with components of mucus layer. This phenomenon has been previously reported with others polymers used as coating materials (Lee et al., 2000; Inchaurraga et al., 2015).

The gastrointestinal-transit studies with radiolabelled nanoparticles revealed that, 2 h post-administration, nanoparticles with the lowest *in vitro* diffusivity (e.g., NPZ and GT-NPZ3) were mainly localized in the stomach mucosa. This fact was particularly intense for GT-NPZ3 (Fig. 2). Conversely, the radioactivity associated to GT-NPZ2 was observed (in a vast majority) in the small intestine of animals. In addition, *in vivo* studies with the fluorescently labelled nanoparticles

corroborated the mucoadhesive properties of NPZ (Fig. 3A and B), as well as the mucus-permeating capabilities of GT coated nanoparticles (Fig. 3C–F). Another important aspect to highlight is that the coating of zein nanoparticles with GT produces nanocarriers capable of entering rapidly in the small intestine, with a low residence time within the stomach. This behavior has been previously observed for pegylated nanoparticles (Inchaurraga et al., 2015) and might be an indication that the "slippery" nanocarriers also offer "targeting" properties for the small intestine.

5. Conclusion

In summary, zein nanoparticles were coated with a Gantrez® AN-thiamine conjugate to yield a continuous and homogeneous corona of about 30 nm thickness. At GT-to-zein ratios up to 5%, the resulting nanoparticles displayed an improved diffusion in intestinal mucus, transforming the mucoadhesive properties of bare nanoparticles into mucus-permeating characteristics. In addition, a good concordance between *in vitro* MPT studies and *in vivo* results has been found.

Declaration of interests

The authors declare that they have no known competing financial interests or personal relationships that could have appeared to influence the work reported in this paper.

The authors declare that they have no known competing financial interests or personal relationships that could have appeared to influence the work reported in this paper.

Acknowledgements

This work was supported by the European Community's Seventh Framework Programme [FP7/2007-2013] ALEXANDER project (grant agreement n° NMP-2011-1.2-2-280761). Furthermore, Laura Inchaurraga acknowledges "Asociación de Amigos" of the University of Navarra for the financial support.

References

Abdulkarim, M., Agulló, N., Cattoz, B., Griffiths, P., Bernkop-Schnürch, A., Borros, S.G., Gumbleton, M., 2015. Nanoparticle diffusion within intestinal mucus: Three-dimensional response analysis dissecting the impact of particle surface charge, size and heterogeneity across polyelectrolyte, pegylated and viral particles. Eur. J. Pharm. Biopharm. 97, 230–238. https://doi.org/10.1016/j.ejpb.2015.01.023.

Arbós, P., Arangoa, M., Campanero, M., Irache, J., 2002. Quantification of the bioadhesive properties of protein-coated PVM/MA nanoparticles. Int. J. Pharm. 242, 129–136. https://doi.org/10.1016/S0378-5173(02)00182-5.

Arbós, P., Campanero, M.A., Arangoa, M.A., Renedo, M.J., Irache, J.M., 2003. Influence of the surface characteristics of PVM/MA nanoparticles on their bioadhesive properties. J. Control. Release 89, 19–30. https://doi.org/10.1016/S0168-3659(03)00066-X.

Areses, P., Agüeros, M.T., Quincoces, G., Collantes, M., Richter, J.Á., López-Sánchez, L.M., Sánchez-Martínez, M., Irache, J.M., Peñuelas, I., 2011. Molecular imaging techniques to study the biodistribution of orally administered 99mTc-labelled naive and ligand-tagged nanoparticles. Mol. Imaging Biol. 13, 1215–1223. https://doi.org/10.1007/s11307-010-0456-0.

Bruno, B.J., Miller, G.D., Lim, C.S., 2013. Basics and recent advances in peptide and protein drug delivery. Ther. Deliv. 4, 1443–1467. https://doi.org/10.4155/tde.13.104.

Cone, R.A., 2009. Barrier properties of mucus. Adv. Drug Deliv. Rev. 61, 75–85. https://doi.org/10.1016/j.addr.2008.09.008.

Cserháti, T., Forgács, E., 2005. Effect of pH and salts on the binding of free amino acids to the corn protein zein studied by thin-layer chromatography. Amino Acids 28, 99–103. https://doi.org/10.1007/s00726-004-0134-0.

Dawson, M., Krauland, E., Wirtz, D., Hanes, J., 2004. Transport of polymeric nanoparticle gene carriers in gastric mucus. Biotechnol. Prog. 20, 851–857. https://doi.org/10.1021/bp0342553.

Ensign, L.M., Cone, R., Hanes, J., 2012. Oral drug delivery with polymeric nanoparticles: The gastrointestinal mucus barriers. Adv. Drug Deliv. Rev. 64, 557–570. https://doi.org/10.1016/j.addr.2011.12.009.

Fonte, P., Araújo, F., Reis, S., Sarmento, B., 2013. Oral insulin delivery: how far are we? J. Diabetes Sci. Technol. 7, 520–531.

Inchaurraga, L., Martín-Arbella, N., Zabaleta, V., Quincoces, G., Peñuelas, I., Irache, J.M., 2015. In vivo study of the mucus-permeating properties of PEG-coated nanoparticles following oral administration. Eur. J. Pharm. Biopharm. 97, 280–289. https://doi.org/10.1016/J.EJPB.2014.12.021.

Inchaurraga, L., Martínez-López, A.L., Cattoz, B., Gri, P.C., Wilcox, M., Pearson, P., Quincoces, G., Peñuelas, I., 2019. The effect of thiamine-coating nanoparticles on their biodistribution and fate following oral administration. Eur. J. Pharm. Sci. 128, 81–90. https://doi.org/10.1016/j.ejps.2018.11.025.

Lai, S.K., Wang, Y.-Y., Hanes, J., 2009. Mucus-penetrating nanoparticles for drug and gene delivery to mucosal tissues. Adv. Drug Deliv. Rev. 61, 158–171. https://doi.org/10.1016/j.addr.2008.11.002.

Larhed, A.W., Artursson, P., Björk, E., 1998. The influence of intestinal mucus components on the diffusion of drugs. Pharm. Res. 15, 66–71.

Lau, J.L., Dunn, M.K., 2018. Therapeutic peptides: Historical perspectives, current development trends, and future directions. Bioorganic Med. Chem. 26, 2700–2707. https://doi.org/10.1016/j.bmc.2017.06.052.

Leader, B., Baca, Q.J., Golan, D.E., 2008. Protein therapeutics: a summary and pharmacological classification. Nat. Rev. Drug Discov. 7, 21–39. https://doi.org/10.1038/nrd2399.

Lee, J.W., Park, J.H., Robinson, J.R., 2000. Bioadhesive-based dosage forms: the next generation. J. Pharm. Sci. 89, 850–866. https://doi.org/10.1002/1520-6017(200007)89:7<850::AID-JPS2>3.0.CO;2-G.

Li, Y.-P., Pei, Y.-Y., Zhang, X.-Y., Gu, Z.-H., Zhou, Z.-H., Yuan, W.-F., Zhou, J.-J., Zhu, J.-H., Gao, X.-J., 2001. PEGylated PLGA nanoparticles as protein carriers: synthesis, preparation and biodistribution in rats. J. Control. Release 71, 203–211. https://doi.org/10.1016/S0168-3659(01)00218-8.

Macierzanka, A., Mackie, A.R., Bajka, B.H., Rigby, N.M., Nau, F., Dupont, D., 2014. Transport of particles in intestinal mucus under simulated infant and adult physiological conditions: impact of mucus structure and extracellular DNA. PLoS One 9, e95274. https://doi.org/10.1371/journal.pone.0095274.

Maher, S., Mrsny, R.J., Brayden, D.J., 2016. Intestinal permeation enhancers for oral peptide delivery. Adv. Drug Deliv. Rev. 106, 277–319. https://doi.org/10.1016/J.ADDR.2016.06.005.

Menzel, C., Holzeisen, T., Laffleur, F., Zaichik, S., Abdulkarim, M., Gumbleton, M., Bernkop-Schnürch, A., 2018. In vivo evaluation of an oral self-emulsifying drug delivery system (SEDDS) for exenatide. J. Control. Release 277, 165–172. https://doi.org/10.1016/J.JCONREL.2018.03.018.

Mert, O., Lai, S.K., Ensign, L., Yang, M., Wang, Y.-Y., Wood, J., Hanes, J., 2012. A poly (ethylene glycol)-based surfactant for formulation of drug- loaded mucus penetrating particles. J Control Release J Control Release. Febr. 10, 455–460. https://doi.org/10.1016/j.jconrel.2011.08.032.

Mitragotri, S., Burke, P.A., Langer, R., 2014. Overcoming the challenges in administering biopharmaceuticals: formulation and delivery strategies. Nat. Publ. Gr. 13. https://doi.org/10.1038/nrd4363.

Muheem, A., Shakeel, F., Jahangir, M.A., Anwar, M., Mallick, N., Jain, G.K., Warsi, M.H., Ahmad, F.J., 2016. A review on the strategies for oral delivery of proteins and peptides and their clinical perspectives. Saudi Pharm. J. 24, 413–428. https://doi.org/10.1016/J.JSPS.2014.06.004.

Mura, S., Hillaireau, H., Nicolas, J., Kerdine-Römer, S., Le Droumaguet, B., Deloménie, C., Nicolas, V., Pallardy, M., Tsapis, N., Fattal, E., 2011. Biodegradable nanoparticles meet the bronchial airway barrier: how surface properties affect their interaction with mucus and epithelial cells. Biomacromolecules 12, 4136–4143. https://doi.org/10.1021/bm201226x.

Netsomboon, K., Bernkop-Schnürch, A., 2016. Mucoadhesive vs. mucopenetrating particulate drug delivery. Eur. J. Pharm. Biopharm. 98, 76–89. https://doi.org/10.1016/J.EJPB.2015.11.003.

Ojer, P., Salman, H., Da Costa Martins, R., Calvo, J., López De Cerain, A., Gamazo, C., Lavandera, J.L., Irache, J.M., 2010. Spray-drying of poly(anhydride) nanoparticles for drug/antigen delivery. J. Drug Deliv. Sci. Technol. 20, 353–359. https://doi.org/10.1016/S1773-2247(10)50059-5.

Peñalva, R., Esparza, I., González-Navarro, C.J., Quincoces, G., Peñuelas, I., Irache, J.M., 2015. Zein nanoparticles for oral folic acid delivery. J. Drug Deliv. Sci. Technol. 30, 450–457. https://doi.org/10.1016/j.jddst.2015.06.012.

Pereira de Sousa, I., Cattoz, B., Wilcox, M.D., Griffiths, P.C., Dalgliesh, R., Rogers, S., Bernkop-Schnürch, A., 2015. Nanoparticles decorated with proteolytic enzymes, a promising strategy to overcome the mucus barrier. Eur. J. Pharm. Biopharm. 97, 257–264. https://doi.org/10.1016/J.EJPB.2015.01.008.

Perera, G., Zipser, M., Bonengel, S., Salvenmoser, W., Bernkop-Schnürch, A., 2015. Development of phosphorylated nanoparticles as zeta potential inverting systems. Eur. J. Pharm. Biopharm. 97, 250–256. https://doi.org/10.1016/j.ejpb.2015.01.017.

Philibert, J., 2005. One and a half century of diffusion: fick, Einstein, before and beyond. Diffus. Fundam. 4, 1–19. https://doi.org/10.1093/ajcn/29.2.205.

Remington, G., Rodriguez, Y., Logan, D., Williamson, C., Treadaway, K., 2013. Facilitating Medication Adherence in Patients with Multiple Sclerosis. Int. J. MS Care 15, 36–45. https://doi.org/10.7224/1537-2073.2011-038.

Rohrer, J., Partenhauser, A., Hauptstein, S., Gallati, C.M., Matuszczak, B., Abdulkarim, M., Gumbleton, M., Bernkop-Schnürch, A., 2016. Mucus permeating thiolated self-emulsifying drug delivery systems. Eur. J. Pharm. Biopharm. 98, 90–97. https://doi.org/10.1016/j.ejpb.2015.11.004.

Rouzes, C., Gref, R., Leonard, M., De Sousa Delgado, A., Dellacherie, E., 2000. Surface modification of poly(lactic acid) nanospheres using hydrophobically modified dextrans as stabilizers in an o/w emulsion/evaporation technique. J. Biomed. Mater. Res. 50, 557–565.

Schneider, C.S., Xu, Q., Boylan, N.J., Chisholm, J., Tang, B.C., Schuster, B.S., Henning, A., Ensign, L.M., Lee, E., Adstamongkonkul, P., Simons, B.W., Wang, S.-Y.S., Gong, X., Yu, T., Boyle, M.P., Suk, J.S., Hanes, J., 2017. Nanoparticles that do not adhere to mucus provide uniform and long-lasting drug delivery to airways following inhalation. Sci. Adv. 3.

Shah, R.B., Patel, M., Maahs, D.M., Shah, V.N., 2016. Insulin delivery methods: past, present and future. Int. J. Pharm. Investig. 6, 1–9. https://doi.org/10.4103/2230-973X.176456.

Skalko-Basnet, N., 2014. Biologics: the role of delivery systems in improved therapy. Biologics 8, 107–114. https://doi.org/10.2147/BTT.S38387.

Suk, J.S., Lai, S.K., Boylan, N.J., Dawson, M.R., Boyle, M.P., Hanes, J., 2011. Rapid transport of muco-inert nanoparticles in cystic fibrosis sputum treated with *N* -acetyl cysteine. Nanomedicine 6, 365–375. https://doi.org/10.2217/nnm.10.123.

Usmani, S.S., Bedi, G., Samuel, J.S., Singh, S., Kalra, S., Kumar, P., Ahuja, A.A., Sharma, M., Gautam, A., Raghava, G.P.S., 2017. THPdb: database of FDA-approved peptide and protein therapeutics. PLoS One 12, 1–12. https://doi.org/10.1371/journal.pone.0181748.

Yildiz, H.M., McKelvey, C.A., Marsac, P.J., Carrier, R.L., 2015. Size selectivity of intestinal mucus to diffusing particulates is dependent on surface chemistry and exposure to lipids. J. Drug Target. 23, 768–774. https://doi.org/10.3109/1061186X.2015.1086359.

Yin, N., Brimble, M.A., Harris, P.W., Wen, J., 2014. Enhancing the Oral Bioavailability of Peptide Drugs by using Chemical Modification and Other Approaches 4. doi: 10.4172/2161-0444.1000227.

Yoncheva, K., Lizarraga, E., Irache, J.M., 2005. Pegylated nanoparticles based on poly (methyl vinyl ether-co-maleic anhydride): preparation and evaluation of their bioadhesive properties. Eur. J. Pharm. Sci. 24, 411–419. https://doi.org/10.1016/j.ejps.2004.12.002.